Kent Academic Repository

Fleischhauer, F., Feuchter, T., Leick, L., Rajendram, R. and Podoleanu, A. (2018) *Impact of absorption in the top layer of a two layer sample on spectroscopic spectral domain interferometry of the bottom layer.* In: Podoleanu, Adrian G.H. and Bang, Ole, eds. 2nd Canterbury Conference on OCT with Emphasis on Broadband Optical Sources. Proceedings of SPIE . SPIE. ISBN 978-1-5106-1674-5.

Impact of absorption in the top layer of a two layer sample on spectroscopic spectral domain interferometry

F. Fleischhauer[1,2,*], T. Feuchter[1], L. Leick[1], R. Rajendram[3, 4] and A. Podoleanu[2]
[1]NKT Photonics A/S, Blokken 84, 3460 Birkeroed, Zealand, Denmark
[2]University of Kent, Applied Optics Group, CT2 7NH Canterbury, United Kingdom
[3]NIHR Moorfields Biomedical Research Centre, Moorfields Eye Hospital, London, United Kingdom
[4]UCL Institute of Ophthalmology, University College London, London, United Kingdom

ABSTRACT

Spectroscopic spectral domain interferometry and spectroscopic optical coherence tomography combine depth information with spectrally-resolved localised absorption data. These additional data can improve diagnostics by giving access to functional information of the investigated sample. One possible application is measuring oxygenation levels at the retina for earlier detection of several eye diseases.

Here measurements with different hollow glass tube phantoms are shown to measure the impact of the on top placed absorbing layer on the precision of reconstructed attenuation spectra of deeper layers.

Measurements show that a superior absorber has no impact on the reconstructed absorption spectrum. Even when diluting the concentration so far that an incorrect absorption maximum is reconstructed, is no influence of the on top placed absorber measured.

Keywords: (110.4500) Optical coherence tomography; (300.6170) Spectroscopy - Spectra

1. INTRODCUTION

Spectroscopic optical coherence tomography (SOCT) is based on spectroscopic spectral domain interferometry (Sp-SDI) [1-3]. By manipulating different parts of the recorded spectrum, access is gained on spectral changes over depth that can be subsequently used for investigation of changes in absorption. Recent publications [4, 5] have shown that Sp-SDI can be employed for measuring oxygen tension at the retina by detecting the different concentrations of deoxygenated and oxygenated haemoglobin in the retinal blood vessels.

SDI uses broadband light and measures the interference pattern as a function of wavelength. A Fourier transform is employed to reconstruct the depth information [3].

For Sp-SDI, the channelled spectrum is divided into narrow spectral windows and a Fourier transform is applied to each of such windows. As every spectral window of each OCT channel is centred at a different wavelength, a link between the information acquired and the wavelength can be established. By comparing the depth information of each spectral window with that of other spectral windows, a relative attenuation spectrum can be reconstructed.

2. SET-UP

The set-up used consists of a supercontinuum source from NKT Photonics A/S (SuperK EXU6 OCT) with a spectral filter (NKT Photonics, SuperK SPLIT VIS/IR). The output of the supercontinuum source is coupled into a wideband fibre coupler from Gould Fiber Optics (45-W 62 56-50-2 22 6 1) with a central wavelength of 560 nm and a bandwidth of ±100 nm, which splits the light evenly in the two interferometer arms. The reference arm consists of a fibre launching with an achromatic lens from Thorlabs Inc. (AC127-019-A-ML), hardware dispersion compensation (Thorlabs, N-BK7), a focusing lens (Thorlabs, AC127-025-A-ML) and a mirror. The sample arm consists of the same fibre launching and focusing lens. The back scattered light from the two interferometer arms is combined again by the fibre coupler and is connected to a commercially available CobraVIS spectrometer from Wasatch Photonics, covering a bandwidth between 430 to 730 nm. The combination of the supercontinuum source used and the spectrometer enables detection of light in the range of 465 to 730 nm.

---

[*] ftf3@kent.ac.uk; phone: +44 1227 82 3772

The axial resolution is measured to be 1.49 µm, which is larger compared to theory. This is caused by unbalanced dispersion left in the interferometer and a Hanning window applied onto the channelled spectrum.

3. MEASUREMENTS

Measurements are performed with two different laser dyes. Rhodamine B, exhibits an absorption maximum at around 542 nm when diluted in ethanol [6], and Malachite green exhibits an absorption maximum at around 616 nm when diluted in water [7]. The two dyes are chosen to exhibit absorption peaks within the used spectrometer range.

Measurements are conducted to investigate the impact of an on top placed absorber on the reconstructed attenuation spectra of an absorber beneath. The on top placed absorber (Rhodamine B) is fixed to a 1:5 concentration and the deeper absorber (Malachite green) concentration is varied in 1:5, 1:10, 1:20 and 1:50 dilutions (volume dilution) and filled into miniature rectangular hollow glass tube from VitroCom (Part # 5005), with an internal gap of 50 µm and a glass wall thickness of 35 µm.

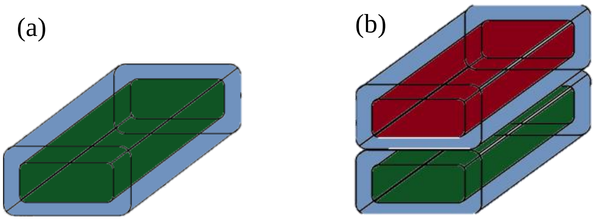

Figure 1: Sketch of single tube (a) and two-layer phantom (b) samples. Dark green corresponds to Malachite green and red represents Rhodamine B.

Phantoms, consisting of two underneath lying tubes are used as a sample in the Sp-SDI and reflections from the glass-air and glass-liquid surfaces is returned and used as depth information.

The recorded channelled spectra are processed before being split into 8 different spectral windows. In a first step is the spectral shape removed, afterwards, is the spectrum linearized to wavenumber. The linearized spectrum is divided into 8 spectral windows by multiplying the spectrum with a Gaussian window at different central wavelengths.

The disagreement between the recorded data and literature values is calculated for each of the eight different central wavelength windows.

The measured data are then normalised to reduce the impact of different reflection amplitudes between different samples. The molar extinction value at the central wavelength of the windows is taken from literature and normalized for comparison purposes. The disagreement is calculated with the formula given in Eq. (1).

$$Disagreement(\lambda_c) = 100 * |\varepsilon(\lambda_c) - a(\lambda_c)| \qquad \text{Eq. (1)}$$

where $|\cdot|$ represents the absolute value, $\varepsilon(\lambda_c)$ the normalised extinction coefficient value at the central wavelength λ_c found in literature and $a(\lambda_c)$ the normalised measured attenuation at the central wavelength of the specific spectral window.

For convenience, the disagreement is calculated in percentage.

For comparison purposes is a single hollow glass tube filled with the same Malachite green concentrations. By comparing the reconstructed attenuation spectra of the two-tube phantom and the single tube sample the impact of the on top placed absorber can be investigated.

4. RESULTS

Figure 3(a) shows a high resolution depth-scan from a two-tube phantom, using the whole spectral bandwidth. The reconstructed attenuation spectra from Rhodamine B in a 1:5 concentration and Malachite green in a 1:20 concentration are shown in Figure 3(b) and 3(c), respectively.

Figure 3 shows that the employed spectral analysis is capable of detecting localised absorption and is capable of distinguishing between 2 different absorber.

The reconstructed normalized attenuation values of single absorber measurement and two tube phantoms inferred are compared to literature and the errors between the two sets of values are calculated in percentages. Figure 4 shows the comparison of the attenuation spectra of Malachite green for different concentrations between literature, single tube and two-tube phantom.

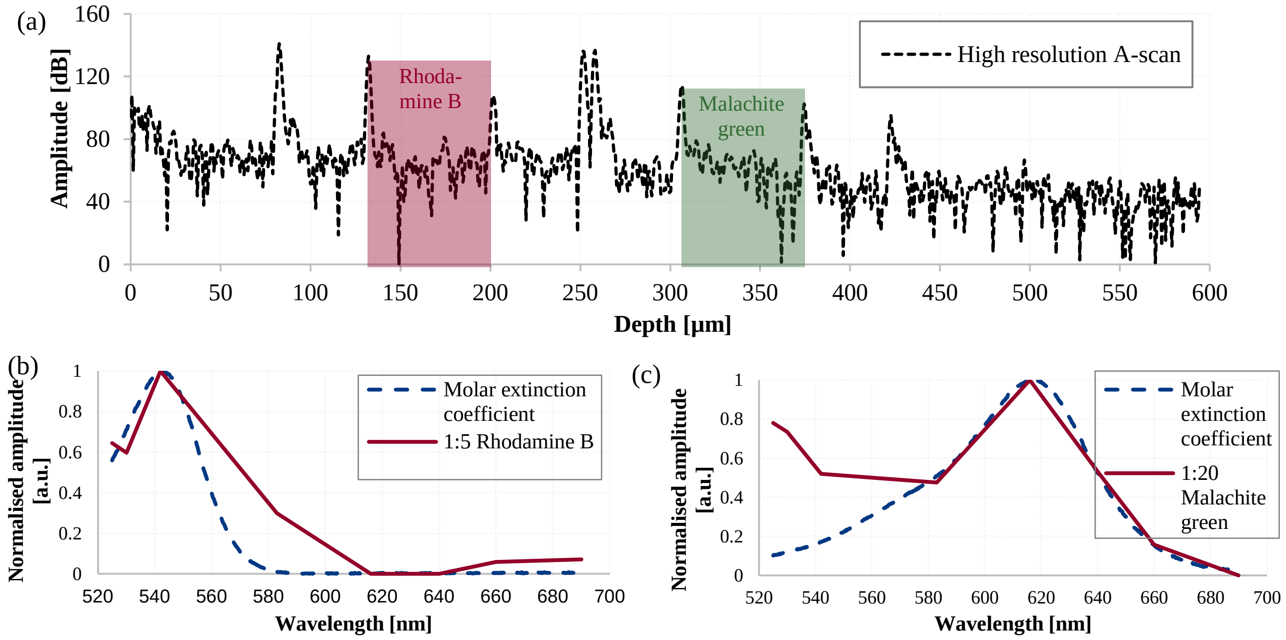

Figure 3: Depth profiles from a phantom containing two different dyes and examples of inferred attenuation spectra obtained with spectroscopic analysis; (a) high resolution A-scan, where the dashed areas indicate the localisation of the two dyes; (b) Inferred attenuation spectrum of the superior tube filled with Rhodamine B with a 1:5 concentration (red solid line) and literature values (blue dashed line); (c) Inferred attenuation spectrum of the inferior tube filled with Malachite green with a concentration of 1:20 (red solid line) and literature values (blue dashed line).

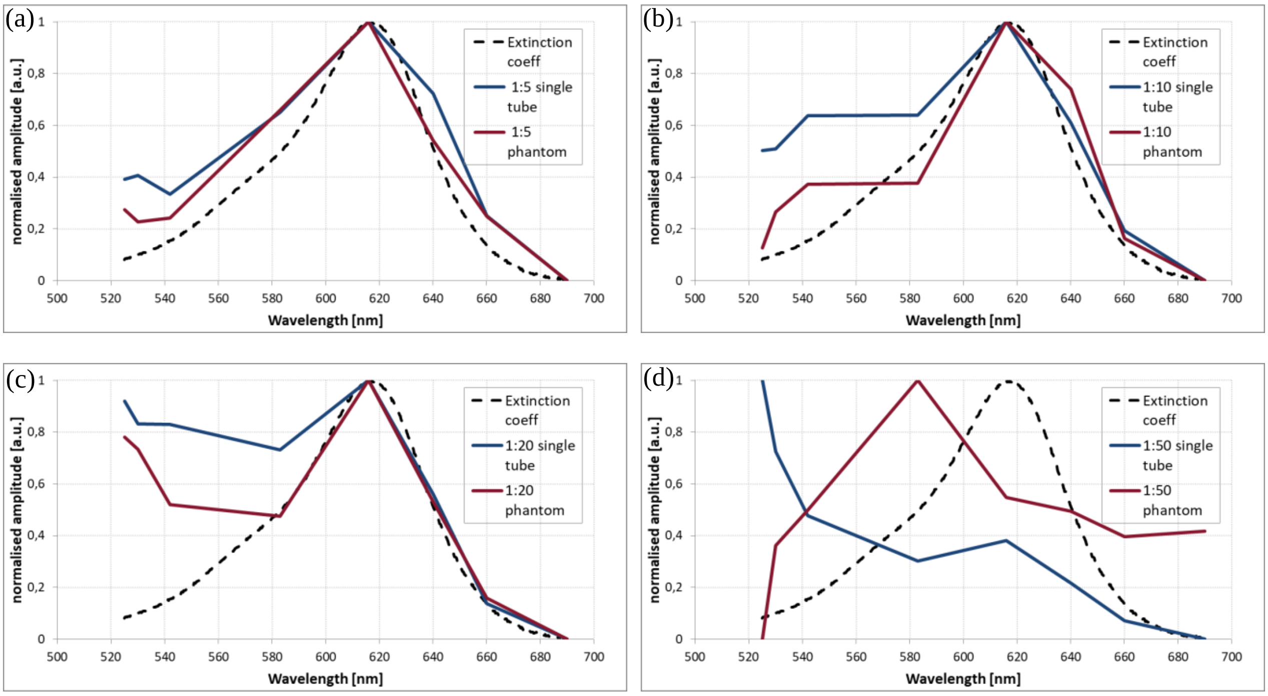

Figure 4: Reconstructed attenuation spectra for different Malachite green concentrations and comparison between literature single tube and phantom measurements. Dashed line represents literature values, Red solid line shows the reconstructed attenuation spectra of the 2 layer phantom and blue solid line shows the reconstructed attenuation spectrum of the single tube measurements. (a) 1:5 concentration, (b) 1:10 concentration, (c) 1:20 concentration and (d) 1:50 concentration.

For Malachite green concentrations of 1:5, 1:10 and 1:20 (Figure 4 a, b, c, respectively) the comparison between experiments and literature values agrees well. Reconstruction of the attenuation spectra measurements of the lowest Malachite green concentration (1:50) fails for both, single tube and two-tube phantom measurements, and the reconstructed attenuation spectra differs significantly from the literature values. With decreased absorber concentration becomes the agreement between literature values and reconstructed attenuation spectrum worse. In case of an impact of the on top placed absorber on the reconstructed attenuation spectrum, a second absorption peak at 542 nm (maximum absorption peak of Rhodamine B) should appear in the two-tube phantom but should not be present in the single tube measurements. No such peak appears in any of the measured attenuation spectra, when compared to the single tube sample, where no on top absorber infers the absorption. Even when the spectroscopic analysis fails to reconstruct the correct attenuation spectrum no influence of the on top placed absorber can be measured.

5. CONCLUSION

The measurements show that Sp-SDI can be used to infer absorption profiles of absorbers placed deep to superficial absorbers. The accuracy in inferring the spectral profile of a deeper absorber of variable concentration placed underneath a different absorber was evaluated and no impact of the on top placed absorber is measured, even when reducing the concentration so that the spectroscopic analysis fails to correctly reconstruct the absorption spectrum.

ACKNOWLEDGEMENTS

F. Fleischhauer, T. Feuchter, L. Leick and A. Podoleanu acknowledge the UBAPHODESA Marie Curie European Industrial Doctorate 607627.
A. Podoleanu is also supported by the NIHR Biomedical Research Centre at Moorfields Eye Hospital NHS Foundation Trust and the UCL Institute of Ophthalmology and the Royal Society Wolfson Research Merit Award.

REFERENCES

[1] N. Bosschaart, M. C. G. Aaldrers, T. G. van Leeuwen and D. J. Faber, “Spectral domain detection in low-coherence spectroscopy,” Biomed. Opt. Express **3**(9), 2263-2272 (2012)
[2] U. Morgner, W. Drexler, F. X. Kärtner, X. D. Li, C. Pitris, E. P. Ippen and J. G. Fujimoto, “Spectroscopic optical coherence tomography,“Opt. Lett. **25**, 11-113 (2000)
[3] A.L. Oldenburg, C. Xu and S. A. Boppart, “Spectroscopic Optical Coherence Tomography and Microscopy,“ IEEE J. Sel. Topics Quantum Electron., **13**(6), 1629-1640 (2007)
[4] J. Yi, W. Liu, S. Chen, V. Backman, N. Sheibani, C. M. Sorenson, A. A. Fawzi, R.A. Linsenmeier and H. F. Zhang, Visible light optical coherence tomography measures retinal oxygen metabolic response to systemic oxygenation, Light: Science & Applications **2015**(4), 1-10 (2015)
[5] S. P. Chong, C. W. Merkle, C. Leahy, and V. J. Srinivasan, "Cerebral metabolic rate of oxygen (CMRO$_2$) assessed by combined Doppler and spectroscopic OCT," Biomed. Opt. Express **6**, 3941-3951 (2015)
[6] Rhodamine B in ethanol absorption spectrum, 05.03.2012, Scott Prahl, Oregon Medical Laser Center, URL: http://omlc.org/spectra/PhotochemCAD/html/009.html (accessed: 05.01.2016)
[7] Malachite green in water absorption spectrum, 05.03.2012, Scott Prahl, Oregon Medical Laser Center, URL: http://omlc.org/spectra/PhotochemCAD/html/030.html (accessed: 05.01.2016)